Efficient and Accurate Measurement of Absorption Cross Section of a Lossy Object in Reverberation Chamber Using Two One-Antenna Methods

Zhihao Tian, *Student Member*, *IEEE*, Yi Huang, *Senior Member*, *IEEE*, Yaochun Shen, and Qian Xu

***Abstract*— The averaged absorption cross section (ACS) of a lossy object can be measured in a reverberation chamber (RC). Conventionally, the measurement is conducted in the frequency domain and it requires two antennas with known efficiency. In this paper, two one-antenna methods are presented – one is in the frequency domain and the other is in the time domain. In the frequency domain, by using the enhanced backscatter effect, the measurement setup is greatly simplified and only one antenna with known efficiency is required. In the time domain, the measurement can be conducted rapidly and accurately using just one antenna and the source stir technique by considering the robustness of the chamber decay time; moreover, the RC can be replaced by a suitable electrically large conducting cavity, which will greatly reduce the hardware requirement. It is found that, the time domain approach is superior to the frequency domain approach in many aspects. The new measurement methods are efficient and accurate while the system requirements and setup are simpler than the conventional ones.**

***Index Terms*—Absorption cross section, reverberation chamber, electrically large cavity, one-antenna method, frequency domain, time domain, source stir.**

I. Introduction

THE reverberation chamber (RC), also known as a mode-stirred chamber, can be characterized as an electrically large shielded metallic enclosure, which is designed to work in an "over mode" condition, with typically an asymmetric rotating paddle to change the boundary conditions of the chamber [1]. Thus, a statistical environment is created inside the chamber and it offers a unique test facility. The RC is becoming prevalent as an alternative test facility for both electromagnetic and electromagnetic compatibility (EMC) measurements. It is currently used for a wide range of measurement applications, such as antenna efficiency measurement [2-4], shielding characterization of equipment and materials [5-8] and EMC radiated emission and immunity tests [1, 9].

Manuscript received November 22, 2015.

Z. Tian, Y. Huang, Y. Shen and Q. Xu are with the Department of Electrical Engineering and Electronics, The University of Liverpool, Liverpool, L69 3GJ, UK (e-mail: zhihao.tian@liv.ac.uk; yi.huang@liv.ac.uk; Y.C.Shen@liverpool.ac.uk; qian.xu@liv.ac.uk).

Recently, it has been shown that the RC can also be used to measure the averaged absorption cross section (ACS) of a lossy object, which is averaged over all angles of incidence and polarization [10, 11]. The measurement of the ACS of a lossy object is required for many applications including the characterization of the effect of lossy objects in multipath environments such as interiors of mass transit vehicles or aircraft loaded with cargoes or passengers [12], biometrics electromagnetic exposure studies such as human's specific absorption rate (SAR) [13].

The ACS of a lossy object is defined as the ratio of the power dissipated in the object to the power density of the incident plane wave. The averaged statistic power transfer function of an RC is proportional to its quality factor. The ACS contribution to the quality factor was derived mathematically in [14], which offers an opportunity to measure the averaged ACS of an object from the quality factor of the reverberation chamber.

For ACS measurement, the common approach is to place a transmitting antenna inside a chamber along with a generic receiving antenna and extract the power transfer function by measuring the transmission coefficient S_{21}, and reflection coefficients S_{11} and S_{22}. The problem with this approach is that it requires two antennas with known efficiency - this could be a problem in reality. An alternative technique given in [15] is to use the coherence bandwidth which is estimated from the complex correlation function of the loaded and unloaded chambers, but it has its own approximations and limitations because of the ambiguity introduced by selecting the threshold for determining the bandwidth of the modes. In this paper, we propose to use both the frequency domain and the time domain information to obtain ACS. Our method requires only one antenna and provides an accurate measurement of ACS without the above-mentioned limitations and approximations.

This paper is organized as follows. Section II contains the formula derivation for the one-antenna method for the measurement of ACS in the frequency domain and in the time domain. Section III presents the measurement setup and comparison of measured ACS using different methods. Section IV presents the convergence properties of the proposed methods. The discussions and conclusions of this work are given in the final section.

II. THEORY

The quality factor (Q) of the RC is a key quantity in calculating the ACS of lossy objects. Generally, in an electrically large cavity, Q is defined as:

$$Q = \omega U_s / P \tag{1}$$

where ω is the angular frequency, U_s is the steady state energy in the cavity and P is the dissipated power.

When the cavity is unloaded, i.e., there are no lossy objects within the chamber, the dissipated power can be written as the summation of three items [14]:

$$P_u = P_{wall} + P_{ant} + P_{lkg} \tag{2}$$

where P_u is the total power dissipated under the unloaded scenario, P_{wall} is the power dissipated in the cavity walls, P_{ant} is the power consumed by the antennas and P_{lkg} is the power leakage due to any apertures of the cavity.

By substituting (2) to (1), we can write the following equation for the inverse of Q:

$$Q_u^{-1} = Q_{wall}^{-1} + Q_{ant}^{-1} + Q_{lkg}^{-1} \tag{3}$$

where

$$Q_{wall} = 3V/2\mu_r S\delta \tag{4}$$

It is determined by the loss due to the finite conductivity of the walls of the cavity, V is the chamber volume, S is the inner surface area of the cavity, μ_r is the relative permeability of the wall, δ is the skin depth of the wall [14].

$$Q_{ant} = 16\pi^2 V/m\lambda^3 \tag{5}$$

is the contribution due to receiving antenna. m is the mismatch factor of the antenna and λ is the wavelength [14]. In addition,

$$Q_{lkg} = 4\pi V/\lambda\langle\sigma_{lkg}\rangle \tag{6}$$

is the contribution from the apertures of the cavity. $\langle\sigma_{lkg}\rangle$ is the averaged transmission cross section [14].

When the cavity is loaded with lossy objects, the total dissipated power can be rewritten as:

$$P_l = P_{wall} + P_{ant} + P_{lkg} + P_{ACS} \tag{7}$$

where P_l is the total power dissipated under the loaded scenario, P_{ACS} is the power loss of the lossy objects.

The corresponding inverse of Q becomes:

$$Q_l^{-1} = Q_{wall}^{-1} + Q_{ant}^{-1} + Q_{lkg}^{-1} + Q_{ACS}^{-1} \tag{8}$$

The contribution of the ACS to the cavity Q can be expressed as:

$$Q_{ACS} = 2\pi V/\lambda\langle\sigma_{ACS}\rangle \tag{9}$$

If we want to know the averaged absorption cross section of a lossy object, we can determine it from its contribution to chamber Q from (9):

$$\langle\sigma_{ACS}\rangle = \frac{2\pi V}{\lambda} Q_{ACS}^{-1} \tag{10}$$

where $\langle\cdot\rangle$ indicates average with respect to the incidence angle and polarization.

From (3), (8) and (10), the averaged absorption cross section $\langle\sigma_{ACS}\rangle$ can be re-written in terms of the measured loaded and unloaded chamber Q factors Q_l and Q_u:

$$\langle\sigma_{ACS}\rangle = \frac{2\pi V}{\lambda}(Q_l^{-1} - Q_u^{-1}) \tag{11}$$

Thus we still need two pieces of information, Q_l and Q_u, in order to determine $\langle\sigma_{ACS}\rangle$. Basically, the chamber Q factor can be measured either in the frequency domain or in the time domain. In the frequency domain, the chamber Q can be evaluated from the averaged net power transfer function T by using Hill's formulas in [14]. In the time domain, the chamber Q can be obtained from the chamber decay time τ [2, 16-18]. Both the averaged net power transfer function and the chamber decay time can be extracted using only one antenna [2]. In the following part of this section, we are going to derive the formulas required for the one-antenna method to determine the ACS of lossy objects within the RC both in the frequency domain and in the time domain.

A. Frequency Domain

In the frequency domain, the averaged statistic power transfer function of an RC is proportional to its quality factor Q_{FD} [14].

$$Q_{FD} = \frac{16\pi^2 V}{\lambda^3}\frac{\langle P_r\rangle}{P_t} \tag{12}$$

where $\langle P_r\rangle$ is the average received power, P_t is the transmitted power in the chamber, and $\langle\cdot\rangle$ means average over all stirrer positions. The second item on the right hand side of (12) is related to the *S*-parameter measured using a vector network analyzer (VNA) as:

$$\frac{\langle P_r\rangle}{P_t} = \langle|S_{21}|^2\rangle \tag{13}$$

A simple measurement of this *S*-parameter would account for contributions from dissipative and mismatch loss of antennas. The contributions from the stirred (energy that interacts with the paddles) and unstirred energy (energy that does not interact with the paddles) in the chamber are included as well. Thus, $\langle|S_{21}|^2\rangle$ can be regarded as the uncalibrated chamber transfer function. By calibrating out the dissipative and mismatch loss

of antennas we can remove the unstirred contributions of *S*-parameters. The net power transfer function T can be extracted as [19]:

$$T = \frac{\langle |S_{21,s}|^2 \rangle}{(1-|\langle S_{11}\rangle|^2)(1-|\langle S_{22}\rangle|^2)\eta_1^{rad}\eta_2^{rad}} \tag{14}$$

where $S_{21,s}$ is the stirred part of S_{21} which can be obtained by the vector average subtraction [20]:

$$S_{*,s} = S_* - \langle S_* \rangle \tag{15}$$

$\langle\cdot\rangle$ means the averaged value of the *S*-parameters, as defined earlier, but here it is linked to the stir method (mode stir, frequency stir, source stir, *etc.*), η_1^{rad} and η_2^{rad} are the radiation efficiency of antenna 1 and antenna 2 that are used in the measurement, respectively.

Substituting (12), (13) and (14) into (11), the averaged ACS $\langle\sigma_{ACS}\rangle$ can be determined from the net power transfer function with and without the lossy objects (T_l, T_u):

$$\langle\sigma_{ACS}\rangle = \frac{\lambda^2}{8\pi}(T_l^{-1} - T_u^{-1}) \tag{16}$$

Typically, the net power transfer function is measured with two low-loss antennas using (14). The radiation efficiency of the two antennas (η_1^{rad}, η_2^{rad}) should be known in advance, or, for a rough measurement, we could assume the efficiency to be unity, which will actually introduce systematic errors.

For a well performed RC, the enhanced backscatter constant [2, 21]

$$e_b = \sqrt{\langle |S_{11,s}|^2 \rangle \langle |S_{22,s}|^2 \rangle} \Big/ \langle |S_{21,s}|^2 \rangle = 2 \tag{17}$$

Assuming two identical antennas are used in the measurement, we have $\langle |S_{11,s}|^2 \rangle = \langle |S_{22,s}|^2 \rangle = 2\langle |S_{21,s}|^2 \rangle$. Now, equation (14) can be expressed as:

$$T = \frac{\langle |S_{11,s}|^2 \rangle}{2(1-|\langle S_{11}\rangle|^2)^2(\eta_1^{rad})^2} \tag{18}$$

Thus, only one antenna is needed to complete this measurement, and we only need to know the radiation efficiency of one antenna, which will greatly simplify the measurement.

B. Time Domain

The time domain method is realized by performing the measurement in the frequency domain and then transforming the results to the time domain. In the time domain, the loaded and unloaded chamber Q can be determined from the chamber time constant. [2, 22] have shown $Q_{TD} = \omega\tau$, ω is the angular frequency and τ is the chamber decay time. The loaded and unloaded Q can be written as:

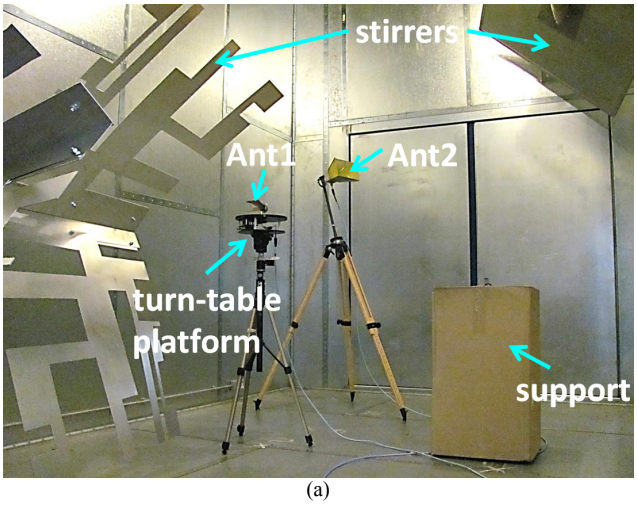

(a)

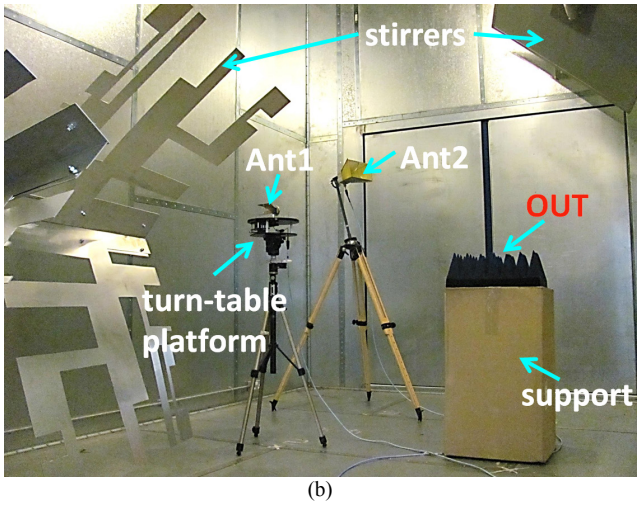

(b)

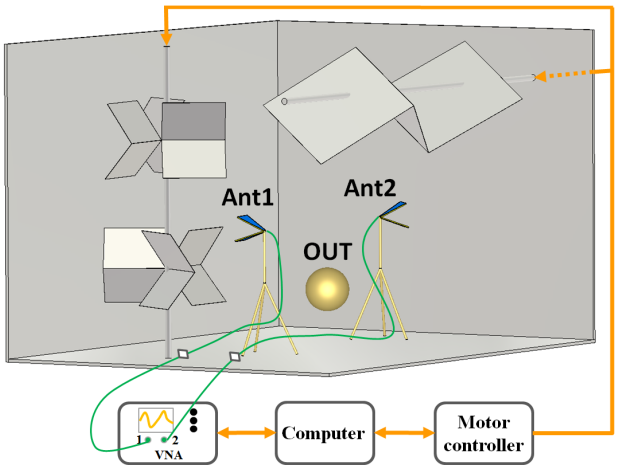

(c)

Fig. 1. ACS measurement setup in the RC: (a) unloaded scenario, (b) loaded scenario, (c) measurement system.

$$Q_l = \omega\langle\tau_l\rangle \text{ and } Q_u = \omega\langle\tau_u\rangle \tag{19}$$

where $\langle\tau_l\rangle$ is the loaded chamber time constant and $\langle\tau_u\rangle$ is the unloaded chamber time constant. If we substitute (19) into (11), we can also obtain the ACS in the following form [22]:

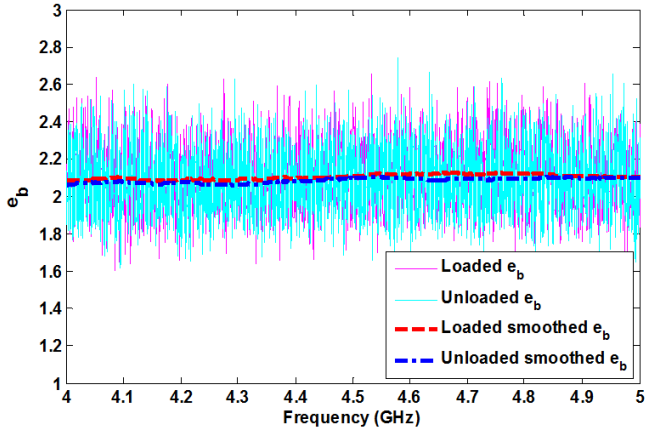

Fig. 2. e_b under the loaded and unloaded scenarios.

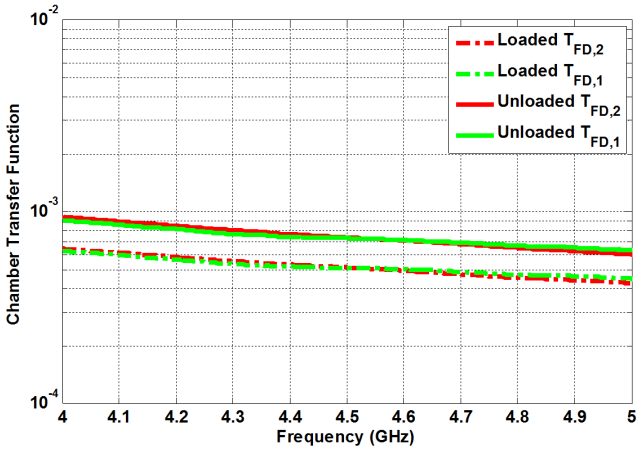

Fig. 3. The measured chamber transfer function using one-antenna and two-antenna methods under loaded and unloaded scenarios.

$$\langle \sigma_{ACS} \rangle = \frac{V}{c}(\langle \tau_l \rangle^{-1} - \langle \tau_u \rangle^{-1}) \tag{20}$$

where c is the speed of light in free space. This technique requires the knowledge of the chamber decay time τ. To obtain τ, we first need to obtain the power delay profile of the RC from the inverse Fourier transform (IFT) of S_{11}. Because the time domain power in the RC decays exponentially, thus τ can be obtained from the slope of ln(power) in the time domain. The details for extracting τ from the S-parameters can be found in [16]. Compared with the frequency domain method, the time domain method is simpler and more accurate because we do not require the knowledge of the antenna efficiency and the systematic error caused by antenna efficiency estimation can be avoided.

III. Measurement

To validate the proposed methods, measurements were performed from 4 to 5 GHz in our RC which has a size of 3.6 m × 4 m × 5.8 m. It has two mode-stir paddles: the vertical one is mounted in a corner while the horizontal one is set close to the ceiling. Two double-ridged waveguide horn antennas were used as antenna 1 (SATIMO® SH 2000) and antenna 2 (Rohde & Schwarz® HF 906). Antenna 1 was mounted on a turn-table platform to introduce source stir positions and connected to port

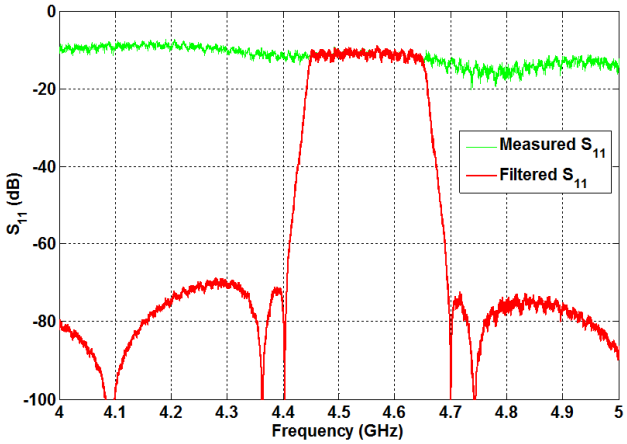

(a)

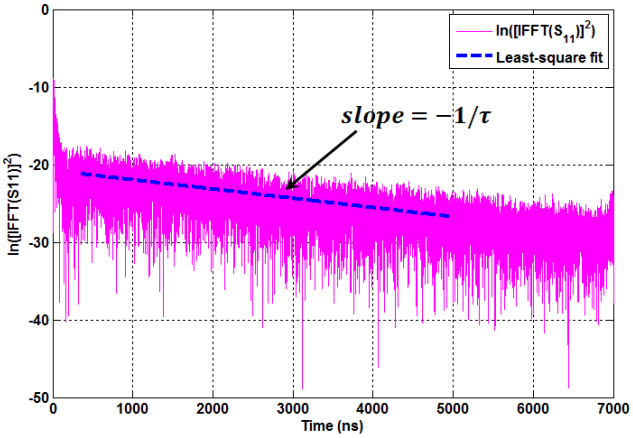

(b)

Fig. 4. Extracting τ from S_{11}: (a) measured S_{11} and filtered S_{11}, (b) time domain response: ln([IFFT(S_{11})]^2) and least-square fit.

1 of a VNA via a cable running through the bulkhead of the chamber, and antenna 2 was connected to port 2 of the VNA via another cable through the bulkhead of the chamber. During the measurement, the turn-table platform was moved stepwise to 3 source stir positions (20 degree for each step), at each source stir position the two paddles were moved simultaneously and stepwise to 100 positions (3.6 degree for each step). At each mode stir position and for each source stir position, a full frequency sweep was performed by the VNA and the S-parameters were collected. Thus, for each frequency, we have 300 stir positions (3 source stir positions, and 100 mode stir positions for each source stir position). A piece of RF absorber was selected as an object under test (OUT). The measurement setups without and with the OUT are shown in Fig. 1 (a) and Fig. 1 (b), respectively. The whole measurement system is shown in Fig. 1 (c).

The measurement procedure is given as follows.

Step 1: Calibrate the VNA including the cables according to the standard calibration procedure.

Step 2: Place the two antennas, the turn-table platform and the support (excluding the OUT) inside the RC.

Step 3: Connect antenna 1 to port 1 of the VNA and antenna 2 to port 2 of the VNA, and collect the full S-parameters for each stir position.

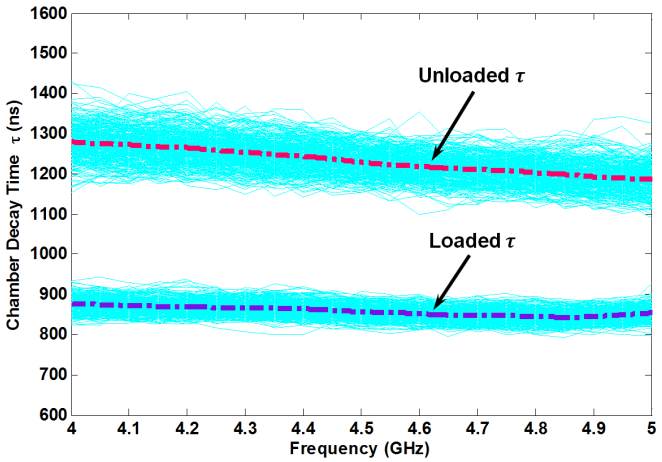

Fig. 5. The measured chamber decay time using one-antenna method under loaded and unloaded scenarios.

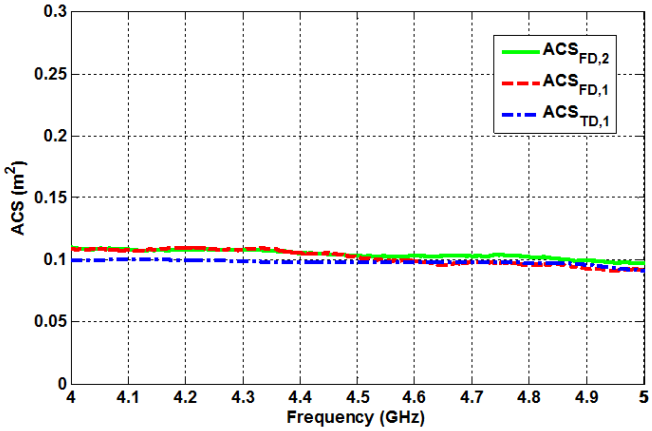

Fig. 6. The measured ACS of the OUT.

Step 4: Keep the previous measurement setup unchanged and place the OUT on the support, and repeat Step 3.

In this measurement, 10,001 points were sampled in the frequency range from 3.8 to 5.2 GHz. The ACS of the OUT was calculated using the conventional two-antenna method ($ACS_{FD,2}$), the one-antenna method in the frequency domain ($ACS_{FD,1}$) and the one-antenna method in the time domain ($ACS_{TD,1}$), respectively. The first subscript "FD" or "TD" is used to indicate that the measurement is conducted in the frequency domain or in the time domain, respectively, and the second subscript "1" or "2" is used to indicate that one antenna or two antennas were used in the measurement. In the frequency domain, the enhanced backscatter coefficients (e_b) under the loaded and unloaded scenarios are obtained and shown in Fig. 2. We can see that they are very close to 2, which means the RC is well stirred and measurement setup is reasonable [23]. The chamber transfer functions using one antenna method ($T_{FD,1}$) and two-antenna method ($T_{FD,2}$) under loaded and unloaded scenarios are shown in Fig. 3. As can be seen, the chamber transfer function is reduced when the chamber is loaded because of the increase of the power loss. $T_{FD,1}$ is very close to $T_{FD,2}$ for both loaded and unloaded scenarios, which manifests the effectiveness of the one-antenna method in the frequency domain. In the time domain, we use a band-pass elliptic filter of order 10 to filter S_{11} with 200 MHz bandwidth, as shown in Fig. 4(a), and then the IFFT is applied to the filtered S_{11}. Since the time domain power decays exponentially ($e^{-t/\tau}$) in the RC, the least-square fit is applied to ln(power) to obtain the slope, and τ can be extracted by getting the negative inverse of the slope. To avoid the fit error caused by the noise level, only part of the signal is used for least-square fit, as shown in Fig. 4. By sweeping the center frequency of the filter, τ at different center frequencies are obtained. The measured chamber decay time using one-antenna method under loaded and unloaded scenarios are depicted in Fig. 5. The thin cyan curves are the measured τ for different stir samples and the thick dash curves are the averaged τ for all samples. As expected, the chamber decay time is reduced when the chamber is loaded. Another thing to be noted is that τ is very robust in the full frequency span, i.e., τ does not vary much for different stir samples. The reason can be explained as follows: the chamber decay time τ is determined by the chamber loss. For a given frequency, the chamber loss will vary due to the change of the paddle positions and the change of the chamber modes. When the number of resonant modes is massive (1,657,518 modes in 4 GHz in our RC according to Weyl's formula [22]), the positions of the peaks and troughs of the resonant mode will not change much for different boundary conditions, and the loss variation is relatively small for different paddle positions. Hence, the chamber decay time is very robust. As shown in Fig. 5, under the unloaded scenario, the variation between the τ for one sample and the averaged τ is within about ±10%. And under the loaded scenario, the variation is within about ±5%. It is easy to understand, when the RC is loaded, the majority of the power is consumed by the lossy objects, the power loss is not sensitive to the boundary condition of the RC, and hence the loaded τ is more robust than the unloaded τ. The robustness of the chamber decay time actually offers an opportunity to extract τ by merely a few number of stir samples, thus the ACS can be measured rapidly and accurately, which will be detailed later. The ACS measurement results are shown in Fig. 6. In the frequency domain, 200 MHz frequency stir is adopted. The efficiency of antenna 1 and antenna 2 in 4-5 GHz are 78% and 95%, respectively. It can be seen clearly that the measured ACSs using the three methods are all around 0.1 m^2 and the maximum variation is within 10%.

IV. Convergence Property

The convergence properties of the three methods are also studied. The root-mean-square-error (RMSE) of the measured ACS from 4-5 GHz with different numbers of stir positions to the ACS measured with 300 stir positions is adopted to evaluate the convergence, and the algorithm is expressed as:

$$\mathrm{RMSE}_i = \sqrt{\frac{\sum_{j=1}^{N}(\mathrm{ACS}_{i,j} - \mathrm{ACS}_{M,j})^2}{N}} \quad (i = 1,2,\cdots,M) \quad (21)$$

where i is the number of stir positions, M is the maximum number of stir positions, j is the frequency sampling point number, N is the number of frequency sampling points in 4-5 GHz. In our case, $M = 300$ and $N = 7143$. The calculated results are shown in Fig. 7. As can be seen, the convergence speeds of the one-antenna method and the two-antenna method in the

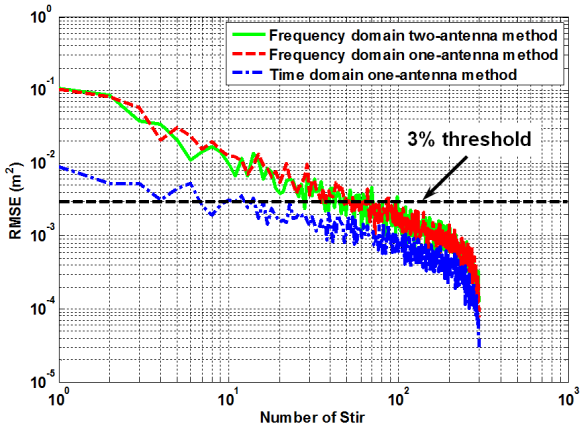

Fig. 7 The RMSE with the increase of the number of stir positions for different methods.

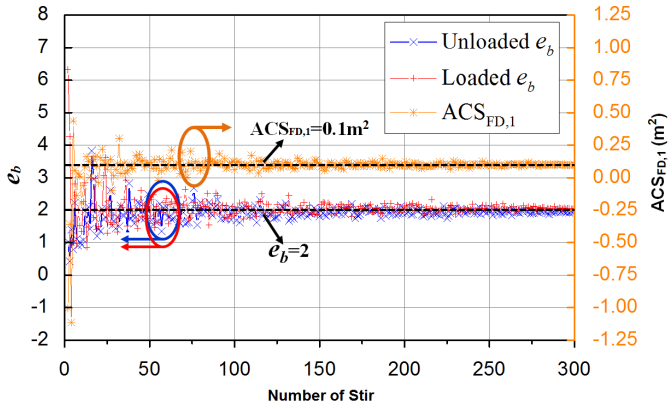

Fig. 8 The convergence behavior of the measured e_b and $ACS_{FD,1}$ @ 4.5 GHz.

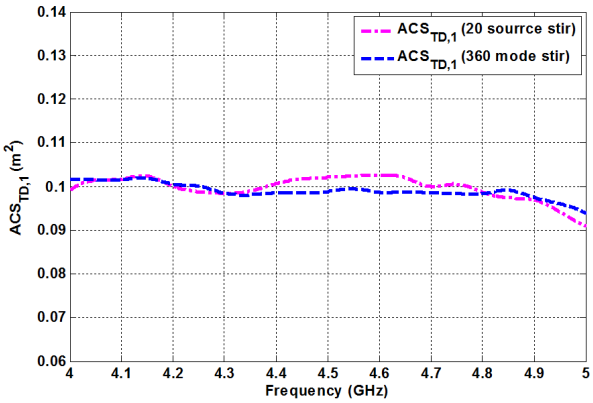

Fig. 9 The comparison of the measured ACS in the time domain with 20 source stir positions and 360 mode stir positions.

frequency domain are close but the time domain method converges faster than the frequency domain methods. This is because the chamber decay time τ is not sensitive to the boundary conditions and only depends on the overall loss of the RC. While the chamber transfer function and e_b depend on how well the RC is stirred. Thus, $ACS_{TD,1}$ converges faster than $ACS_{FD,1}$ and $ACS_{FD,2}$. It is worth mentioning that, in the time domain, the RMSE is always below 10% (compared with the averaged ACS in the full frequency span, about 0.1 m^2 from Fig. 6) and drops below 3% after 15 stir positions. However, in the frequency domain, the one-antenna method and the two-antenna method have similar convergence behaviour, the

TABLE I
COMPARISON OF DIFFERENT MEASUREMENT METHODS

Measurement method	Number of antennas needed	Measurement time	Measurement facility needed
FD two-antenna method	2	approx. 8 hours	reverberation chamber
FD one-antenna method	1	approx. 8 hours	reverberation chamber
TD one-antenna method (mode stir)	1	approx. 7 minutes	reverberation chamber
TD one-antenna method (source stir)	1	approx. 7 minutes	electrically large cavity

RMSEs are always above 10% before the first 10 stir positions and drop down slowly afterwards. They are below 3% after 100 stir positions. As implied in (17) and (18), the one-antenna method in the frequency domain requires $e_b = 2$. Inaccurate results may be obtained if e_b deviates from 2. To show the influence of the deviation of e_b from 2 to the validity of the measurement in the frequency domain based on one-antenna approach, we have checked the convergence behavior of the measured e_b (under both loaded and unloaded scenarios) and $ACS_{FD,1}$ at 4.5 GHz, as shown in Fig. 8. The $e_b = 2$ level and $ACS_{FD,1} = 0.1$ m^2 level are marked out with dash lines. As can be seen, at the first dozens of stir, the deviation of e_b from 2 fluctuates drastically, the measured ACS is unreliable. However, with the increase of the number of stir, e_b converges to 2 gradually. The convergence behavior of $ACS_{FD,1}$ is very similar to e_b. After about 150 stir, the variation of e_b from 2 becomes small (within 10% variation) and the measured $ACS_{FD,1}$ becomes stable (it converges to 0.1 m^2). That means that the accuracy of the frequency domain one-antenna approach highly depends on $e_b = 2$, i.e., how well the chamber is stirred.

Considering the robustness of the chamber decay time and the fast convergence property of the time domain method, the measurement setup can be further simplified by using an electrically large conducting cavity, i.e., an RC is not necessary. To verify this idea, the paddles of the RC were set stationary, therefore, no mode stir was introduced during the measurement, and thus the RC would merely act as an electrically large cavity. To extract the correct τ of the electrically large cavity, a simple source stir was introduced by rotating the turn-table platform. Based on the convergence speed of the one-antenna method in the time domain, 20 source stir positions was adopted in our measurement. The turn-table platform was moved stepwise to 20 source stir positions (18 degree for each step). A double-ridged waveguide horn antenna (SATIMO® SH 2000) was mounted on the turn-table platform and connected to port 1 of a VNA via a cable running through the bulkhead of the cavity. The measurement procedure was similar to that in the RC. The cavity decay time with and without OUT was extracted from S_{11}. The measurement results are shown in Fig. 9. As can be seen, the results from the mode stir and source stir are in good agreement. The difference is within 4% and the whole measurement time for the source stir was about 7

minutes while the measurement time for the mode stir was more than 8 hours, which means that the ACS can be measured in the time domain rapidly and accurately. The major contribution to the measurement time is the damping time of the turn-table platform between the steps and the time of transferring data from the VNA to the computer. The measurement time of this method is comparable with that of the rapid method proposed in [24] and therefore, it is quite suitable for applications requiring discriminations between subjects due to its high accuracy and short measurement time. It should be pointed out that the cavity should be large enough to support sufficient cavity modes to ensure enough independent samples to be obtained at the lowest frequency of the measurement, or the OUT could not fully "submerge" into the field-uniform area and the measurement result could be wrong. This is the main consideration for the selection of the size of the conducting cavity in the measurement.

V. Discussions and Conclusions

In this paper, we have presented one-antenna methods for determining the ACS of the OUT in the frequency domain and in the time domain. The commonly used RC technique for determine the ACS of the OUT requires two antennas and the radiation efficiency of the two antennas should be known. In this paper, we first presented the one-antenna method in the frequency domain which requires only one antenna (with known efficiency) by making use of enhanced backscatter effect. Thus, the measurement setup was simplified. Then, we presented the one-antenna method in the time domain which needs no knowledge of the efficiency of the antenna. Experimental setup was illustrated and measurement results were presented. It seems that the measured ACSs by the three methods are in good agreement. We investigated the robustness of the chamber decay time and the convergence speed of the three methods and found that the time domain method converges much faster than the frequency domain methods. A rapid and accurate measurement can be achieved in the time domain based on this finding by using source stir technique, which makes it quite suitable for human absorption and exposure measurement. Furthermore, in the time domain approach, the RC can be replaced by a suitable electrically large conducting cavity, which will greatly reduce the hardware requirement. The method was validated in the RC by setting the paddles stationary and the results agree well with that measured in the RC using mode stir. The comparison of the measurement methods mentioned above is shown in Table I. It is demonstrated that the time domain method is much more efficient and its hardware requirement is much lower than the frequency domain method.

There are some points that need to be emphasized. Firstly, the proposed methods presented in this paper assume that the RC was well stirred. When the RC is not well stirred, the OUT could not fully "submerge" in the field-uniform area. The measured chamber transfer function and chamber decay time will be inaccurate, hence the measured ACS will be of considerable errors. Secondly, the antennas used in the measurement should be of high efficiency in the time domain method, i.e., the losses in the RC are dominated by the chamber wall loss and OUT loss rather than by the losses of the antennas used in the measurement. Otherwise, the power will not decay exponentially and chamber decay time cannot be extracted correctly. However, in the frequency domain, the antennas used do not have to be of high efficiency because the antenna efficiency has been calibrated out in the net power transfer function. Thirdly, during the measurement, the OUT should be set far away from the antennas to avoid the proximity effect [25]. Last but not least, the calculation of the ACS requires the difference in the net power transfer function (in the frequency domain) or the chamber decay time (in the time domain) with and without the OUT, as seen in (16) and (20). If the loss of the OUT is too small compared with that of the chamber itself, it will be very difficult for the chamber to distinguish the difference of the loss (i.e., the difference of the Q factors between loaded and unloaded scenarios), which will result into the inaccuracy of the measurement. However, for most of the applications, like the measurement of the human body absorption cross section, the loss of the OUT is normally large enough for the chamber to see and thus the ACS can be accurately calculated.

Future work may include the application of the proposed one-antenna method for real applications, such as the measurement of the absorption cross section of human bodies in the RC.

References

[1] *Electromagnetic Compatibility (EMC) part 4-21: Testing and measurement techniques-Reverberation chamber test methods*, IEC 61000-4-21, 2003.

[2] C. L. Holloway, H. A. Shah, R. J. Pirkl, W. F. Young, D. A. Hill, and J. Ladbury, "Reverberation chamber techniques for determining the radiation and total efficiency of antennas," *IEEE Trans. Antennas Propag*., vol. 60, no. 4, pp. 1758-1770, Apr. 2012.

[3] C. L. Holloway, R. Smith, C. Dunlap, R. Pirkl, J. Ladbury, W. Young, B. Hansell, M. Shadish, and K. Sullivan, "Validation of a one-antenna reverberation-chamber technique for estimating the total and radiation efficiency of an antenna," in *Proc. IEEE Int. Symp. on Electromagnetic Compatibility*, Aug. 2012, pp. 205-209.

[4] H. G. Krauthauser and M. Herbrig, "Yet another antenna efficiency measurement method in reverberation chambers," in *Proc. IEEE Int. Symp. on Electromagnetic Compatibility*, Jul. 2010, pp. 536-540.

[5] *IEEE Standard Method for Measuring the Effectiveness of Electromagnetic Shielding Enclosures*, IEEE Standard 299, 2006.

[6] C. L. Holloway, D. A. Hill, M. Sandroni, J. M. Ladbury, J. Coder, G. Koepke, A. C. Marvin, and Yuhui He, "Use of Reverberation Chambers to Determine the Shielding Effectiveness of Physically Small, Electrically Large Enclosures and Cavities," *IEEE Trans. Electromagn. Compat*., vol.50, no.4, pp. 770-782, Nov. 2008.

[7] D. Fedeli, G. Gradoni, V. M. Primiani, and F. Moglie, "Accurate analysis of reverberation field penetration into an equipment-level enclosure," *IEEE Trans. Electromagn. Compat.*, vol. 51, no. 2, pp. 170–180, May 2009.

[8] G. B. Tait, C. Hager, M. B. Slocum, and M. O. Hatfield, "On Measuring Shielding Effectiveness of Sparsely-Moded Enclosures in a Reverberation Chamber," *IEEE Trans. Electromagn. Compat.*, vol. 55, no. 2, pp. 231-240, Apr. 2013.

[9] H. G. Krauthäuser, "On the measurement of total radiated power in uncalibrated reverberation chambers," *IEEE Trans. Electromagn. Compat*., vol. 49, no. 2, pp. 270-279, 2007.

[10] U. Carlberg, P.-S. Kildal, A. Wolfgang, O. Sotoudeh, and C. Orlenius, "Calculated and measured absorption cross sections of lossy objects in reverberation chamber," *IEEE Trans. Electromagn. Compat*., vol. 46, no. 2, pp. 146-154, May 2004.

[11] E. Amador, M. Andries, C. Lemoine, P. Besnier, “Absorbing material characterization in a reverberation chamber,” in *Proc. IEEE Int. Symp. on Electromagn. Compat.*, Sept. 2011, pp. 117-122.
[12] G. C. R. Melia, M. P. Robinson, I. D. Flintoft, A. C. Marvin, and J. F. Dawson, "Broadband Measurement of Absorption Cross Section of the Human Body in a Reverberation Chamber," *IEEE Trans. Electromagn. Compat*., vol. 55, no. 6, pp. 1043-1050, Dec. 2013.
[13] A. Bamba, D. P. Gaillot, E. Tanghe, G. Vermeeren, W. Joseph, M. Lienard, and L. Martens, "Assessing Whole-Body Absorption Cross Section For Diffuse Exposure From Reverberation Chamber Measurements," *IEEE Trans. Electromagn. Compat*., vol. 57, no. 1, pp. 27-34, Feb. 2015.
[14] D. A. Hill, M. T. Ma, A. R. Ondrejka, B. F. Riddle, M. L. Crawford, and R. T. Johnk, "Aperture excitation of electrically large, lossy cavities," *IEEE Trans. Electromagn. Compat*., vol. 36, no. 3, pp. 169-178, Aug. 1994.
[15] M. I. Andries, P. Besnier, and C. Lemoine, "On the prediction of the average absorbing cross section of materials from coherence bandwidth measurements in reverberation chamber," in *Proc. IEEE Int. Symp. on Electromagn. Compat.*, Sept. 2012, pp. 1-6.
[16] C. L. Holloway, H. A. Shah, R. J. Pirkl, K. A. Remley, D. A. Hill, and J. Ladbury, "Early Time Behavior in Reverberation Chambers and Its Effect on the Relationships Between Coherence Bandwidth, Chamber Decay Time, RMS Delay Spread, and the Chamber Buildup Time," *IEEE Trans. Electromagn. Compat*., vol. 54, no. 4, pp. 714-725, Aug. 2012.
[17] D. L. Green, V. Rajamani, C. F. Bunting, B. Archambeault, and S. Connor, “One-port time domain measurement technique for quality factor of loaded and unloaded cavities,” in *Proc. IEEE Int. Symp. on Electromagn. Compat.*, Aug. 2013, pp. 747-750.
[18] C. Vyhlidal, V. Rajamani, C. F. Bunting, P. Damacharla, and V. Devabhaktuni, “Estimation of absorber performance using reverberation techniques and artificial neural network models,” in *Proc. IEEE Int. Symp. on Electromagn. Compat.*, Aug. 2015, pp. 897-901.
[19] S. J. Boyes, P. J. Soh, Y. Huang; G. A. E. Vandenbosch, N. Khiabani, "Measurement and Performance of Textile Antenna Efficiency on a Human Body in a Reverberation Chamber," *IEEE Trans. Antennas Propag*., vol.61, no.2, pp. 871-881, Feb. 2013.
[20] C. L. Holloway, D. A. Hill, J. M. Ladbury, P. F. Wilson, G. Koepke, and J. Coder, "On the Use of Reverberation Chambers to Simulate a Rician Radio Environment for the Testing of Wireless Devices," *IEEE Trans. Antennas Propag*., vol.54, no.11, pp. 3167-3177, Nov. 2006.
[21] J. M. Ladbury and D. A. Hill, "Enhanced Backscatter in a Reverberation Chamber: Inside Every Complex Problem is a Simple Solution Struggling to Get Out," in *Proc. IEEE Int. Symp. on Electromagnetic Compatibility*, Jul. 2007, pp. 1-5.
[22] D. A. Hill, *Electromagnetic Fields in Cavities: Deterministic and Statistical Theories*. New York: IEEE Press, 2009.
[23] C. R. Dunlap, "Reverberation chamber characterization using enhanced backscatter coefficient measurements," Ph.D. dissertation, Dept. of Elect., Comput. and Eng., Univ. of Colorado, Boulder, USA, 2013.
[24] I. D. Flintoft, G. C. R. Melia, M. P. Robinson, J. F. Dawson, and A. C. Marvin. "Rapid and accurate broadband absorption cross-section measurement of human bodies in a reverberation chamber," *Meas. Sci. Technol*., vol. 26, no. 6, pp. 65701-65709, Jun. 2015.
[25] W. T. C. Burger, K. A. Remley, C. L. Holloway, and J. M. Ladbury, "Proximity and antenna orientation effects for large-form-factor devices in a reverberation chamber," in *Proc. IEEE Int. Symp. on Electromagnetic Compatibility*, Aug. 5-9, 2013, pp. 671-676.